Low-temperature features of electron scattering in cadmium

1991 J. Phys.: Condens. Matter 3 10065

(http://iopscience.iop.org/0953-8984/3/51/003)

J. Phys.: Condens. Matter 3 (1991) 10065–10075. Printed in the UK

Low-temperature features of electron scattering in cadmium

A Jaquier†, P A Probst†§, R Stubi†, R Huguenin† and W E Lawrence‡

† Institut de Physique Expérimentale, Université de Lausanne, CH 1015 Lausanne, Switzerland

‡ Department of Physics, Dartmouth College, Hanover NH 03755, USA

Received 28 May 1991, in final form 19 August 1991

Abstract. The scattering rates $\nu(T)$ of various groups of electrons in cadmium have been measured down to 0.25 K using the radio-frequency size effect. For electrons on the third band lens of the Fermi surface, $\nu(T)$ can be analysed below about 2.5 K as the superposition of two terms, αT^2 and βT^3. While the latter is associated with electron–phonon scattering the former component can be attributed to electron–electron scattering. On two triangular orbits in the first and second bands an apparently large T^2 term is observed between 5 and 1.5 K. At lower temperatures $\nu(T)$ drops rapidly suggesting that this behaviour is due to electron–phonon scattering. An explanation for large T^2 terms has been recently proposed by Lawrence *et al* on the basis of Umklapp electron–phonon scattering together with the particular shape of the Fermi surface of cadmium. Simple calculations on these lines are shown to reproduce semi-quantitatively the observed variation of $\nu(T)$ and to aid in the interpretation of another second band orbit.

1. Introduction

Cadmium is well known to be a good candidate in which many aspects of electron transport in metals can be tested. It is not far from a free-electron system, at least over some parts of its Fermi surface (FS) and its metallurgy is well under control so that good single crystals can be reproducibly prepared. Local and orbital averaged scattering rates $\nu(T)$ in Cd have been reported by several authors (Myers *et al* 1974, Naberezhnykh and Tsymbal 1975, Probst *et al* 1980 (PMH)) for groups of charge carriers at various locations on the FS using the radio-frequency size effect (RFSE), a most powerful tool for investigating the temperature-dependent $\nu(T)$. A wealth of temperature behaviours has been discovered (PMH), the origins of which have not yet been completely established. Among the interesting features of the $\nu(T)$ of Cd one can mention the following points:

(i) The $\nu(T)$ of electrons on the FS lens in the third band is anisotropic in magnitude as well as in temperature dependence. In most metals, under good experimental conditions, $\nu(T)$ follows a T^3 law (coefficient β) from electron–phonon (e–p) scattering, sometimes with an additional term αT^2 from electron–electron (e–e) scattering (Stubi *et al* 1988); the anisotropy shows up in the coefficients α and β. In contrast

§ Present address: H H Wills Physics Laboratory, University of Bristol, Bristol BS8 1TL, UK.

0953-8984/91/5110065+11$03.50

$\nu(T)$ of the lens electrons in Cd rises much faster than T^3 above about 2.5 K. PMH successfully used a model which attributes it to the start of intersheet scattering by transverse phonons between the lens and nearby sections of the second band monster of the FS.

(ii) In previous measurements on Cd a T^2 contribution to $\nu(T)$, with a coefficient α of the right order of magnitude to attribute it to e–e scattering, could only be found for one particular tilted field orbit, close to the (0001) direction on the FS lens (PMH). For other orbits on the lens $\nu(T)$ was consistent with a term αT^2 having the same value of α. Such a component was, however, difficult to detect unambiguously for various reasons, in particular the deviations from simple T-dependence due to the turning on of strong e–p intersheet scattering and the limited resolution of the measurements comparable with the overall variation of the signal amplitude between 1.2 and 2 K.

(iii) Large quadratic terms αT^2 were observed for orbits on the first and second band sheets of the FS (PMH) which are too large and anisotropic to be attributed to e–e scattering. One observes noticeable differences between the measured values of α, whereas e–e scattering is expected to be isotropic, because of the large angle character of e–e collisions. According to theory, the anisotropy in the coefficient of T^2 from e–e scattering in simple metals should not exceed $V(G)/\epsilon_F$, which is of the order of 10%, where $V(G)$ is the pseudopotential coefficient (Lawrence and Wilkins 1973, Wagner and Bowers 1978). Moreover the reported experimental values of α are, for some orbits, two orders of magnitude larger than those theoretically predicted from e–e scattering and experimentally determined, for instance in the noble metals (Stubi *et al* 1988).

We present here more precise measurements down to 0.25 K, to try to clarify these points. The extension of the temperature range below 1 K should allow the determination of the e–e scattering contribution because e–p scattering has been sufficiently reduced, and should also provide insight into the large T^2 terms mentioned under (iii). Recently Lawrence *et al* (1986) have proposed that they may be due to e–p Umklapp scattering, predicting that $\nu(T)$ would start to drop faster somewhere below 1 K. A simple two-orthogonal-plane-waves (2OPW) calculation of $\nu(T)$ on these lines is presented which shows reasonable agreement with the experimental data.

2. Experimental details

The present measurements were made with the experimental set-up described in Stubi *et al* (1988). Standard modulation techniques are used and the modulated RFSE resonance signal detected by a marginal oscillator is measured with a digital lock-in amplifier (Probst and Collet 1985). The resonance signal arises when a DC magnetic field parallel to the sample surface is such that the sample thickness exactly encompasses the corresponding extremal orbit on the FS. The measurement of the signal amplitude $A(T)$ allows one to determine the orbitally averaged scattering rate $\nu(T)$ from (see Wagner and Bowers 1978):

$$A(T) = A(0)\exp\{-\nu(T)t\} \tag{1}$$

where $A(0)$ is the extrapolated amplitude for $T = 0$ K and t the time for the electrons to cross the sample. The measurements were made down to 250 mK using a dilution refrigerator which makes the determination of $A(0)$ much easier.

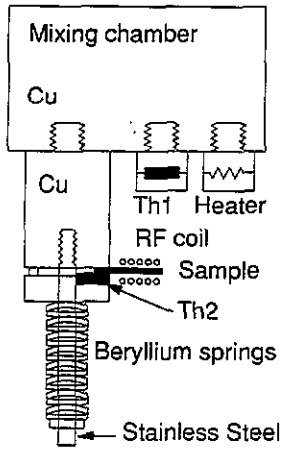

Figure 1. Details of the low-temperature experimental set-up.

Figure 1 shows the location of the sample in the cryostat and the two Ge thermometers Th1 and Th2. The sample temperature is kept constant within a few mK (Probst and Rittener 1989) and the absence of a temperature gradient between Th2 and the sample is checked using the superconducting transition temperature of Cd at 519 mK. The low fields used in RFSE experiments (< 0.05 T) do not affect the properties of the Ge thermometers. The samples are single crystals cut from 6N rods typically 1 cm in diameter with two optically flat surfaces. For these measurements sample Cd1 is 537 μm thick with a normal $\boldsymbol{n}$ parallel to $\langle 11\bar{2}0\rangle$ and sample Cd2 is 240 μm thick with $\boldsymbol{n}$ parallel to $\langle 10\bar{1}0\rangle$. The orientations are chosen so that the electron orbits are symmetrical. The parallelism of the magnetic field relative to the sample surface is achieved by superimposing a small adjustable magnetic field normal to the field of a standard iron magnet.

While our dilution refrigerator has a base temperature of 100 mK, the lowest available temperature in measuring conditions is limited to 250 mK because of the energy input from the oscillator; we have not tried to improve it because the resolution of the detection system would not allow measurements of the small changes in signal amplitudes $A(T)$ below this temperature. $A(T)$ increases typically by 1% on reducing the temperature from 1 to 0.25 K. The digital form of the data allows numerical treatment such as correlation with a reference signal or autocorrelation to improve the noise rejection.

3. Experimental results and discussion

We have chosen to plot the data—$\nu(T)$ being determined from (1)—mostly as $\nu(T)/T^2$ against T for the easy identification of any T^2 contribution, the coefficient α of this term being measured by the intercept on the vertical axis.

3.1. Electrons on the third band lens

Figure 2 shows the data in the temperature range from 0.25 to 6 K for electrons on the third band lens of the FS, that is on the extremal circular and elliptical orbits

obtained with $\boldsymbol{B}$ respectively parallel and perpendicular to the c-axis. While the low-temperature points give evidence of a T^2 term superimposed on a T^3 component, the upward curvature above about 2.5 K shows that $\nu(T)$ varies much more rapidly than T^3 at high temperature. This agrees with previous measurements by Myers *et al* (1972) and by PMH. The absence of a T^5-like temperature dependence below 1 K, as can be more clearly seen in the insert of figure 2, indicates that ineffective e–p scattering due to the smallness of the phonon wavevectors at low temperature cannot be invoked for interpreting deviations from the usual T^3 law. The theoretical curves calculated with the simple model for intersheet scattering introduced by PMH fit the experimental points well. The intersheet scattering term, due to transitions between the lens and the nearby monster, turns on at about $T_g/10$, where T_g is a gap temperature which depends on the shape of the FS sheets and the velocities of transverse phonons. For the curves in figure 2, T_g is 18 and 16 K for the elliptical and circular orbits respectively.

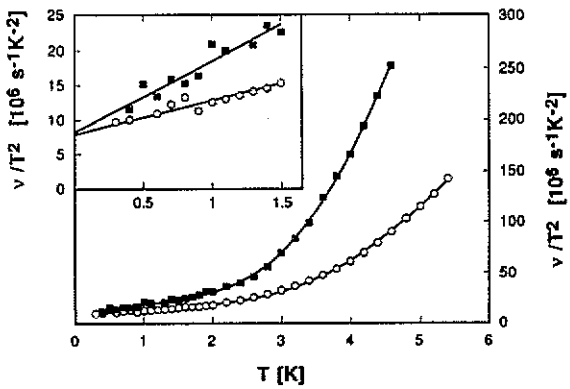

Figure 2. Scattering rate divided by T^2 versus temperature for the elliptical (○) and circular (■) orbits on the FS lens from sample Cd1. The curves are calculated using a simple model (see text). The insert is an expansion of the low-temperature range.

Below 2 K $\nu(T)$ is well described by the sum of a T^2 and a T^3 term (see insert of figure 2):

$$\nu(T)/T^2 = \alpha + \beta T. \tag{2}$$

The intercept with the vertical axis is nearly the same for both orbits and α amounts to approximately 8×10^6 s^{-1} K^{-2}. This is the right order of magnitude at which to attribute this T^2 contribution to e–e scattering, as theoretically estimated by Lawrence and Wilkins (1973) or by MacDonald (1980). In fact Schwartzman (1984 p 115 and foregoing discussion) has estimated a value for Cd of 5.6×10^6 s^{-1} K^{-2} due to the phonon mediated e–e interaction. His estimate applies to the quasiparticle decay rate at the Fermi level, whereas the RFSE measurement provides the energy average, which is larger by the factor 4/3. So the agreement between the theoretical estimate and the experiment appears to be excellent. The isotropy of α also supports this interpretation. The common value of α measured on these two orbits is about 25% larger than that reported by PMH for a tilted field orbit running close to the ⟨0001⟩ direction on the FS lens. This agreement is well within the accuracy of the older data.

3.2. Charge carriers on the first and second band

Three orbits called l, m, n (see figure 2 of PMH) on the first and second band sheets of the FS have been investigated with the magnetic field $\boldsymbol{B}$ tilted by about 10° from the c-axis to avoid an overlap of the resonance signals. The raw data $A(T)$ behave similarly for all these three orbits. As an example $\ln A(T)$ for orbit l is represented as a function of T^2 and T^3 in figure 3(a) showing that neither of the two simple power laws holds. The detailed temperature dependence is, however, different and we have to consider the data for orbits l and m separately from n.

In figures 3(b) and (c), $\nu(T)/T^2$ is plotted against T for the orbits l and m, respectively in the first and second band sheets of the FS. It is seen that the present results do not significantly differ from the data by PMH for a nearby orbit (indicated by the broken curves) with respect to the e–p contribution to $\nu(T)$ measured above 2 K. Also, linear extrapolation of the high-temperature data down to 0 K intercepts the vertical axis nearly at their reported value. However, at temperatures below 1.5 or 2 K, $\nu(T)/T^2$ starts to fall below this extrapolated straight line. This means that the large 0 K value extrapolated from high T data is not related to e–e scattering. Nevertheless the arrows in figure 3(b) show that the low T data are consistent with the value of α determined for the lens orbits.

The same plot for orbit n is shown in figure 4 where it is seen that in this case $\nu(T)$ may indeed be described over the whole temperature interval of our measurements by the superposition of the two contributions αT^2 and βT^3. Here, however, our results disagree significantly with previous data (PMH) which are 20 to 40% above the experimental points in these new measurements, even in the high-temperature range where e–p scattering is dominant. The discrepancy may be partly due to the shape of this particular orbit being very sensitive to the alignment of the magnetic field and sample surface with respect to the FS. One should also mention that in the previous work the measurements were only significant above 1.5 K resulting in a considerable uncertainty in the extrapolation of the amplitude $A(0)$ at 0 K. Because of the much smaller amplitude of the signals here compared to the lens orbits—due to the smaller number of charge carriers involved—it is not easy to assess the precise temperature dependence of $\nu(T)$. The higher resolution in the present measurements and the extension of the temperature range down to 0.25 K obviously allow a better interpretation, in particular of the low-temperature data where the quadratic and cubic terms become comparable.

The intercept of the straight line through the data points in figure 4 amounts to $17\times10^6\ \mathrm{s^{-1}\ K^{-2}}$. It is impossible to determine from the data below about 1 K whether the apparent T^2 term persists to lower temperatures or falls off as it does for the l and m orbits. We would expect that e–e scattering is responsible for about half the apparent T^2 term, based on the lens orbit α values and isotropy arguments. This half should persist down to 0 K, while the other half, due presumably to e–p scattering, should gradually disappear below 1 K. In the next subsection we shall present an estimate for the e–p contribution based on a fit to the data for the triangular orbits. There indeed should be an apparent T^2 dependence above about 1 K due to e–p scattering, at least as large as required for this interpretation to hold.

One might argue against assuming that e–e scattering rates are isotropic, since factor of 2 variations have indeed been found experimentally in transition metals like tungsten (Van der Maas *et al* 1985), and are also predicted by theory (Potter and Morgan 1979). However, Cd is closer to a simple metal, and while variations in α

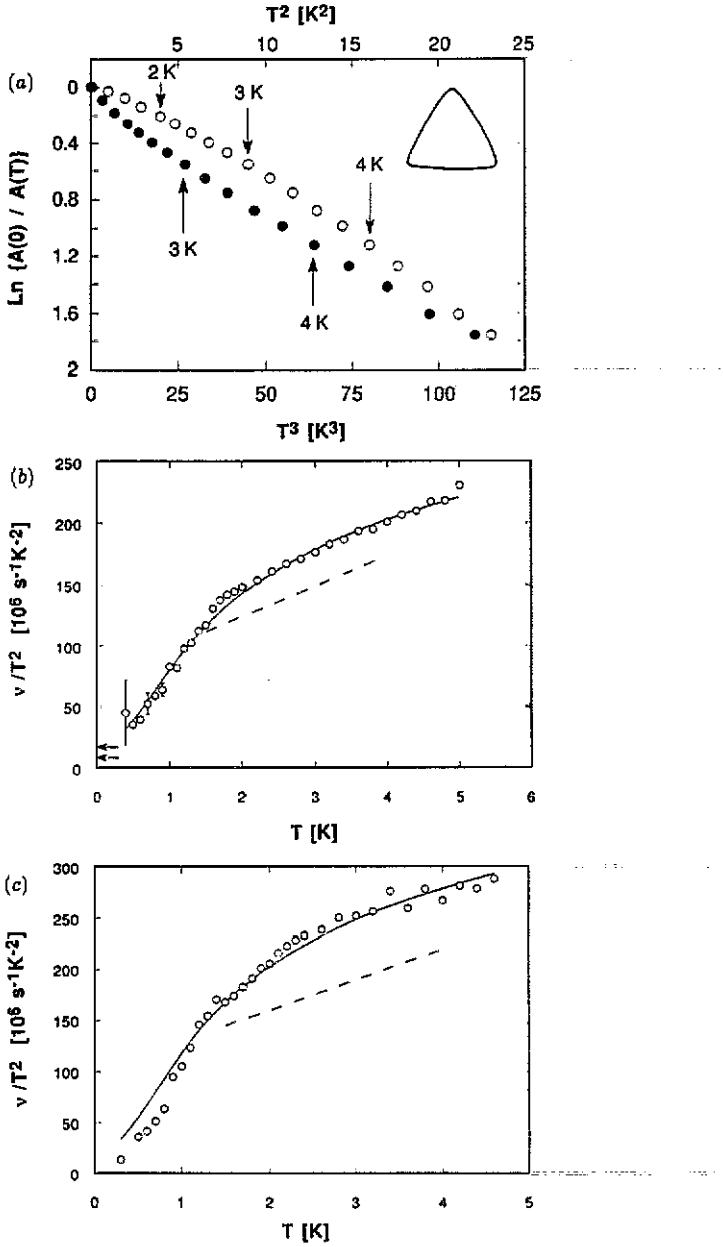

Figure 3. (*a*) The logarithm of the amplitude $A(T)$ of the RFSE signals against T^2 and T^3 for orbit l on the first band of FS from sample Cd2. No simple power law fitted the data. The orbit shape is for the magnetic field $B \parallel c$ and remains approximately triangular for B tilted by 10°. (*b*) The scattering rate divided by T^2 for orbit l. The error bars correspond to changes of ±0.1% on the RFSE signal amplitude. The arrows show the value of the coefficient from e–e scattering on the lens (lower arrow) and n orbit. Data fitted with equation (5) using $\Theta_D = 121$ K, $V(G) = 0.1$ eV and correction terms discussed in the text. The broken curve represents the PMH data for the closest orbit. (*c*) The scattering rate divided by T^2 for orbit m on the second band FS. Data fitted with equation (5) using $\Theta_D = 110$ K, $V(G) = 0.1$ eV and correction terms discussed in the text. The broken curve represents the PMH data for the closest orbit.

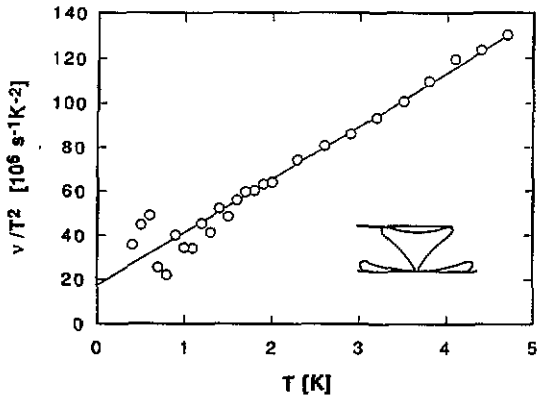

Figure 4. Scattering rate divided by T^2 for orbit n on the second band FS from sample Cd2.

could easily be greater than 10%, it would be surprising if they were as large as a factor of 2. We simply wish to point out that the data so far are consistent with an isotropic α.

A quadratic temperature dependence of $\nu(T)$ has been shown to result (Gantmakher 1974) from e–p scattering in a metal having a very anisotropic cylindrical-like FS, when the phonon wavevectors are much smaller than the length of the cylinder and much larger than its radius. However, the model cannot be used for Cd, the radii of the first and second FS sheets being much too large. Another mechanism has been proposed by Lawrence *et al* (1986) based on e–p Umklapp processes in a metal with FS sheets in close proximity to each other. When the Umklapp-dominated local $\nu(\boldsymbol{k}, T)$ is averaged over the actual electron orbit this model predicts a T^2-like dependence in a limited range of T, with a sharp drop at very low temperature, as we observe in the experiments on orbits l and m. The main results of a simple analytical calculation along the lines suggested in this paper and Lawrence (1991) are briefly outlined in the next subsection.

3.3. A simple model of the e–p $\nu(T)$ for a triangular orbit

$\nu(T)$ for an electron in state $\boldsymbol{k}$ on the FS is given by (Wagner and Bowers 1978)

$$\nu(\boldsymbol{k}) = (2\pi^2\hbar)^{-1} \int \frac{\mathrm{d}S'}{v'} \sum_{\sigma} |g^{\sigma}_{\boldsymbol{k}\boldsymbol{k}'}|^2 \frac{1}{\sinh(\hbar\omega_{q\sigma}/k_{\mathrm{B}}T)} \tag{3}$$

where $\mathrm{d}S'$ is a FS integral over final states $\boldsymbol{k}'$,

$$|g^{\sigma}_{\boldsymbol{k}\boldsymbol{k}'}|^2 = \frac{|\langle \boldsymbol{k}'|\nabla V|\boldsymbol{k}\rangle|^2}{2\rho\omega_{q\sigma}} \tag{4}$$

is the square of the e–p matrix element, $\omega_{q\sigma}$ the phonon frequency at $\boldsymbol{q} = \boldsymbol{k}' - \boldsymbol{k}$, ρ the mass density and V the electron–ion potential. The theoretical $\nu(T)$ to be compared with the experimental data is the average over the appropriate orbit of $\nu(\boldsymbol{k}, T)$ calculated from (3). The model presented here employs a Debye spectrum for phonons in which transverse and longitudinal modes are treated separately, allowing for the dominance of transverse phonons in Umklapp processes. It also employs a

2-OPW model for the three equivalent vertices of a simple equilateral triangle orbit (similar to the orbits l and m where $\nu(T)$ show an anomalous behaviour). Using (3) and the previous arguments we then deduce the expression:

$$\nu(T)/T^2 = \frac{\pi}{6\rho v_F}\frac{k_B^2}{(\hbar c)^3}\frac{G^2V^2(G)}{Q_2}f(T) \tag{5}$$

where c is the transverse sound velocity, G is the reciprocal lattice vector, $V(G)$ the pseudopotential form factor at point G, Q_2 a minimum calliper of the orbit and

$$f(T) = \frac{2}{\pi^2}\int_0^\infty \frac{dz}{\sinh z}[\theta(z - T_1/T)\min(z, T_2/T) + \min(z^2T/aT_1, z, T_2/T)]. \tag{6}$$

This function $f(T)$ expresses departures from the quadratic behaviour of (9) of Lawrence *et al* (1986) below T_1 due to 2-OPW effects and above T_2 due to phase space effects. The parameter a depends on the orbit geometry and is equal to 1.2 for the equilateral triangle. The cut-off temperatures T_1 and T_2 are determined by the characteristic wavevectors of the orbit

$$k_BT_i = \hbar cQ_i \qquad i = 1, 2 \tag{7}$$

the smaller one, Q_1, being the intersheet threshold

$$Q_1 = \frac{4m|V(G)|}{\hbar^2 k_F} \tag{8}$$

and the larger one, Q_2, the orbit calliper.

Substituting the transverse Debye temperature Θ_D for the sound speed, $k_B\Theta_D = \hbar cQ_D$ (with $Q_D \approx k_F$) one can express the two characteristic temperatures for cadmium as

$$\begin{aligned} T_1 &= \Theta_D\left(\frac{4m|V(G)|}{\hbar^2 k_F Q_D}\right) = \Theta_D\left(\frac{2|V(G)|}{E_F}\right) \\ T_2 &= \Theta_D(Q_2/Q_D) = 0.203\Theta_D. \end{aligned} \tag{9}$$

Because the pertinent $V(G)$ is very small for the triangle orbits (about two orders of magnitude less than E_F) the condition for observation of the T^2 behaviour ($T_1/T_2 \ll 1$) is met. With reasonable values of $V(G)$ and Θ_D, equations (5) and (6) yield a large T^2-like contribution for $T \geqslant 2$ K, as shown in figure 5. If the measurements are not made at sufficiently low temperature, extrapolation from the high-temperature data will result in the large values which have been previously published (PMH) for the unphysical coefficient of an apparent T^2 term. However, at low temperatures $\nu(T)$ drops quite rapidly in semi-quantitative agreement with the present measurements below 1.5 K.

Figure 5(a) shows the basic T^2-like dependence (thin curve) arising from (5) and (6) and an additional T^3-like dependence (chain curve) arising from both Umklapp e–p scattering when the pseudopotential form factor is momentum-dependent (broken curve) and the normal e–p scattering is the result of longitudinal phonons. The former effect is determined by the single additional parameter $V'(G) = \partial V(G)/\partial q|_{q=G}$. The basic T^2-like part is evaluated using $|V(G)| = 0.1$ eV and $\Theta_D = 121$ K obtained by a

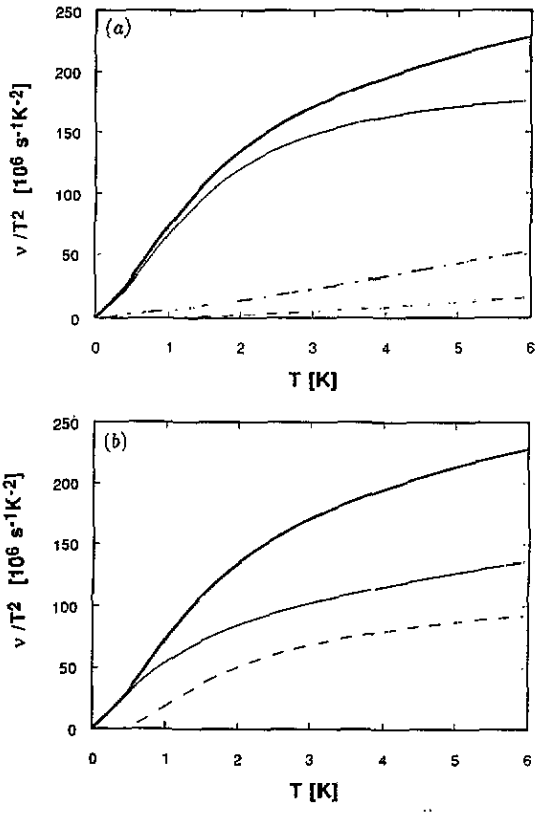

Figure 5. (*a*) Theoretical total scattering rate (bold curve) showing the contribution from equation (5) (thin curve) compared with the Umklapp scattering correction due to $V'(G)$ (broken curve) and normal e–p scattering (chain curve), as described in the text. (*b*) Theoretical total scattering rate (bold curve) consisting of an interband contribution (broken curve) which shows an exponential cut-off at low T, and an intraband (thin curve) contribution (including normal e–p scattering), which goes smoothly from T^2 to T^3 dependence as T is reduced to zero.

fit to the l orbit data. The T^3-like correction is calculated using $|V'(G)| = 0.6$ eV Å and assuming that the normal e–p contribution is the same as that found on the free-electron-like lens orbit produced in the tilted-field geometry (PMH), $\nu_N(T) = 6\times10^6\,T^3\,s^{-1}$. Also, normal scattering accounts for most of the difference (figure 5(*b*)) between intraband (thin curve) and interband (broken curve) contributions above 2 K, where Umklapp scattering is divided about equally between the two, within this model. With regard to the T^2-like behaviour ((5) and (6)), the parameter values quoted by Lawrence *et al* (1986), $|V(G)| = 0.045$ eV, $\Theta_D = 180$ K (determined by the FS fit of Stark and Falicov (1967) and the heat capacity data of Cetas *et al* (1969), respectively) produce almost the identical temperature dependence shown on figure 5(*a*), but with the ordinate scale reduced by about an order of magnitude. On the other hand we might also make a comparison with the parameter values $|V(G)| = 0.35$ eV and $V'(G) = 2.23$ eV Å used by Watts and Mayers (1980) in their analysis of stress-induced changes in extremal FS areas. These larger parameter values were deduced by fitting the same (Stark and Falicov 1967) band structure near symmetry points using the folded-down secular equation. This is analogous in spirit to our use of the 2-OPW

model for low-temperature behaviour of $\nu(T)$. Concerning the large difference between the two approximations to the band structure, it is not surprising that we should have to adjust the parameters mentioned in order to get a close fit quantitatively like those presented on figures 3(b) and 3(c). One would also expect this because of the simplicity of the Debye model and the simple triangle model for the orbit (the actual shape is slightly different as $\boldsymbol{B}$ is 10° from the c-axis). The l and m orbits are in close proximity, and each has more than three zone boundary intersections with very small gaps.

Despite its simplicity, let us apply the model to the n orbit. It predicts a similar feature, but with a much smaller magnitude. The main point is that the amplitude of the apparent T^2 term for $T > T_1$ is proportional to the number of zone boundary intersections (multiplied by the appropriate $V(G)$ squared) divided by the total arc length of the orbit. The appropriate generalization of (5) is to replace $1/Q_2$ by $\sum_G \mathrm{cosec}(\phi_G)/Q_\Gamma$ where Q_Γ is the arc length of the orbit and ϕ_G is the opening angle of the vertex at the intersection with zone boundary G (we omit the $V^2(G)$ factors because the relevant ones are all the same in this case). One may verify the equivalence of these expressions for the equilateral triangle where $\phi_G = \pi/3$. Now the n orbit is not closed, but rather stretches between half-intersections (the orbit extends to one side of the zone boundary, rather than having well-defined segments on both sides). One half-intersection is equivalent to those of the triangle orbits (same $V(G)$ or T_1, and the same ϕ_G), and the other not likely to contribute T^2 because its T_1 is much too large for our temperature range. So in comparison with the triangular orbits, the n orbit has effectively half an intersection rather than three. Since its arc length is about the same as those of the triangles, the model predicts an apparent α value about one sixth as large. This is sufficient to account for the entire apparent T^2 term above 1 K for the n orbit, although we consider it more likely, for the reasons given earlier, that about half of this term arises from e–e scattering. The e–p estimate, while not reliable quantitatively, nevertheless makes this interpretation plausible. The two contributions are difficult to resolve experimentally because of the reduced signal for the n orbit as compared with the lens orbits makes the extrapolation to 0 K much more difficult.

Ultimately, the validity of the theoretical models discussed here and in Lawrence *et al* (1986) cannot be fully established without a microscopic calculation that includes realistic phonon spectra and a full FS. Such a calculation has been performed by Chen (1988) and Chen *et al* (1991), and its results will be reported elsewhere. Apparent T^2-like terms of the order of magnitude of those observed on the triangular orbits are found in a similar temperature interval.

4. Conclusions

We have presented high-resolution measurements of the temperature-dependent $\nu(T)$ for various electron orbits on the FS of Cd between 0.25 and 5 K. For two extremal orbits on the third band lens the existence of a T^2 component has been unambiguously detected with a coefficient α whose value agrees with the theoretical estimate for e–e scattering. This value is the same for the elliptical and circular orbits which further supports this interpretation.

The data for the l and m first and second band orbits show a more complicated temperature dependence. The previously reported large T^2 terms resulting from extrapolation to 0 K of the data above about 2 K are shown to be unphysical, whereas

the low-temperature results are consistent with an e–e coefficient of the order of magnitude obtained on the other orbits. In the temperature range below about 2 K, $\nu(T)$ for these quasi-triangular orbits shows the behaviour predicted by calculations based on a recent model of e–p Umklapp processes using reasonable values for the FS parameters of Cd. In this model the temperature variation of $\nu(T)$ is due to normal scattering at very low temperatures (producing a T^3 dependence), and Umklapp scattering entering and contributing about equally to the total $\nu(T)$ at higher temperatures where the apparent T^2 contribution is seen. This T^2-like behaviour results from the orbital averaging without showing up in the local scattering rate.

Finally, the data for the n orbit on the second band show a T^2 contribution which is about twice that found on the lens orbits, but much less than that found on the triangular orbits. The theoretical model of e–p scattering predicts a temperature dependence similar to that found on the l and m orbits, but with considerably reduced magnitude. Because we expect the e–e contribution to be isotropic and find no evidence to the contrary on other orbits, we suggest that similar contributions arise from e–e scattering and e–p scattering above about 1 K. If this hypothesis is correct, the apparent α value should fall to about half its higher-temperature value as T is reduced well below 1 K. Testing this hypothesis currently appears to be a difficult experimental problem.

References

Cetas T C, Holste J C and Swenson C A 1969 *Phys. Rev.* **182** 679–85

Chen Wei 1988 *PhD Thesis* Indiana University (available from University Microfilms, Ann Arbor, MI, USA)

Chen Wei, Swihart J C and Lawrence W E 1991 *J. Phys.: Condens. Matter* submitted

Gantmakher V F 1974 *Rep. Prog. Phys.* **37** 317–62

Lawrence W E 1991 unpublished

Lawrence W E, Chen Wei and Swihart J C 1986 *J. Phys. F: Met. Phys.* **16** L49 and private communication

Lawrence W E and Wilkins J W 1973 *Phys. Rev.* B **7** 2317–32

MacDonald A H 1980 *Phys. Rev. Lett.* **44** 489–93

Myers A, Porter S G and Thompson R S 1972 *J. Phys. F: Met. Phys.* **2** 24–37

Myers A, Thompson R S and Ali Z 1974 *J. Phys. F: Met. Phys.* **4** 1707–18

Naberezhnykh V P and Tsymbal D T 1967 *Sov. Phys.-JETP Lett.* **5** 263

Potter C and Morgan G J 1979 *J. Phys. F: Met. Phys.* **9** 493–503

Probst P A and Collet B 1985 *Rev. Sci. Instrum.* **56** 466–70

Probst P A, MacInnes W M and Huguenin R 1980 *J. Low Temp. Phys.* **41** 115–56

Probst P A and Rittener J 1989 *HPA* **62** 298–301

Schwartzman K 1984 *PhD Thesis* Dartmouth College available from University Microfilms, Ann Arbor, MI, USA

Stubi R, Probst P A, Huguenin R and Gasparov V A 1988 *J. Phys. F: Met. Phys.* **18** 1211–24; 1988 *J. Phys. F: Met. Phys.* **18** 2429–43

Van der Maas J, Huguenin R and Gasparov V A 1985 *J. Phys. F: Met. Phys.* **15** L271

Stark R W and Falicov L M 1967 *Phys. Rev. Lett.* **19** 795–8

Wagner D K and Bowers R 1978 *Adv. Phys.* **27** 651–746

Watts B R and Mayers J 1980 *J. Phys. F: Met. Phys.* **10** 1693–718